2. Rourke JA, Heslin DJ. Gaucher's disease. *Am J Roentgenol* 1965;94:621–630.
3. Barton NW, Furbish FS, Murray GJ, Garfield M, Brady RO. Therapeutic response to intravenous infusions of glucocerebrosidase in a patient with Gaucher disease. *Proc Natl Acad Sci USA* 1990;87:1913–1916.
4. Grabowski GA, Barton NA, Pastores G, et al. Enzyme therapy in type 1 Gaucher disease: comparative efficacy of mannose-terminated glucocerebrosidase from natural and recombinant sources. *Ann Intern Med* 1995;122:33–39.
5. Starer F, Sargent JD, Hobbs JR. Regression of the radiological changes of Gaucher's disease following bone marrow transplantation. *Br J Radiol* 1987;60:1189–1195.
6. Parker RI, Barton NW, Read EJ, Brady RO. Hematologic improvement in a patient with Gaucher disease on long-term enzyme replacement therapy: evidence for decreased splenic sequestration and improved red blood cell survival. *Am J Hematol* 1991;38:130–137.
7. Ruzal-Shapiro C, Berdon WE, Cohen MD, Abramson SJ. MR imaging of diffuse bone marrow replacement in pediatric patients with cancer. *Radiology* 1991;181:587–589.
8. Kricon ME. Red-yellow marrow conversion: its effect on the location of some solitary bone lesions. *Skel Radiol* 1985;14:10–19.
9. Wang JC, Tobin MS. Mechanisms of extramedullary haematopoiesis in rabbits with saponin-induced myelofibrosis and myeloid metaplasia. *Br J Haematol* 1982;51:277–284.
10. Rosenthal DI, Mayo-Smith W, Goodsitt MM, Doppelt S, Mankin HJ. Bone and bone marrow changes in Gaucher disease: evaluation with quantitative CT. *Radiology* 1989;170:143–146.
11. Rosenthal DI, Barton NW, McKusick KA, et al. Quantitative imaging of Gaucher disease. *Radiology* 1992;185:841–845.

12. Cremin BJ, Davey H, Goldblatt J. Skeletal complications of type I Gaucher disease: the magnetic resonance features. *Clin Cardiol* 1990;41:244–247.
13. Lanir A, Hadar H, Cohen I, Tal Y, Benmair J, Schreiber R, Clouse ME. Gaucher disease: assessment with MR imaging. *Radiology* 1986;161:239–244.
14. Castronovo FP Jr, McKusick KA, Doppelt SH, Barton NW. Radiopharmacology of inhaled ^{133}Xe in skeletal sites containing deposits of Gaucher cells. *Nucl Med Biol* 1993;20:707–714.
15. Dokal IS, Deenmamode M, Lewis SM. Radioisotope studies in monitoring of Gaucher's disease and its treatment. *Clin Lab Haematol* 1989;11:91–96.
16. Katz K, Mechlis-Frish S, Cohen IJ, Horev G, Zaizov R, Lubin E. Bone scans in the diagnosis of bone crisis in patients who have Gaucher disease. *J Bone Joint Surg* 1991;73:513–517.
17. Israel O, Jerushalmi J, Front D. Scintigraphic findings in Gaucher's disease. *J Nucl Med* 1986;27;1557–1563.
18. Cheng TH, Holman BL. Radionuclide assessment of Gaucher's disease. *J Nucl Med* 1978;19:1333–1336.
19. Klingensmith WC III, Tsan MF, Wagner, HN Jr. Factors affecting the uptake of ^{99m}Tc-sulfur colloid by the lung and kidney. *J Nucl Med* 1976;17:681–684.
20. Stadalnik RC. Diffuse lung uptake of Tc-99m-sulfur colloid. *Semin Nucl Med* 1980;10:106–107.
21. Polga JP, Holsten G, Spencer RP. Radiocolloid redistribution and multiple splenic infarcts in myelofibrosis. *Clin Nucl Med* 1983;8:335–336.

Extracorporeal Whole-Blood Immunoadsorption Enhances Radioimmunotargeting of Iodine-125-Labeled BR96-Biotin Monoclonal Antibody

Michael Garkavij, Jan Tennvall, Sven-Erik Strand, Hans-Olov Sjögren, Chen JianQing, Rune Nilsson and Martin Isaksson

Departments of Oncology, Radiation Physics and Immunology, Lund University, Lund, Sweden

This study investigates the efficacy of tumor radioimmunotargeting with ^{125}I-labeled BR96-biotin monoclonal antibody using a new method, whole-blood immunoadsorption (WBIA), based on direct adsorption of unbound monoclonal antibody (MAb) from blood without preceding separation of plasma. **Methods:** Highly tumor-reactive, internalizing, chimeric BR96 MAb of isotype IgG1 binds to a tumor-associated Lewis-type (Le^Y) cell surface antigen. Forty-six Brown Norwegian male rats were inoculated intramuscularly and beneath the liver or kidney capsule with syngeneic rat colon carcinoma BN7005, expressing Lewis-type antigen, and investigated. The rats were injected intravenously with 3.5–4.5 MBq ^{125}I-labeled BR96-biotin. Twenty of the rats underwent WBIA starting 5 or 12 hr after injection. About six blood volumes were passed through an avidin-gel adsorption column during 2 hr. **Results:** By using WBIA, whole-body radioactivity was reduced by 50%, and plasma activity by 85%. Both directly after completion of WBIA and 33 hr later, the activity uptake in tumors manifested only a nonsignificant decrease as compared with corresponding controls (p > 0.05) and had approximately similar time-activity curves. Uptake ratios for tumor (T):bone marrow, T:liver, T:kidney and T:lung were enhanced 2.3- to 3.5-fold in all three tumor models, as compared with controls. The ratio of liver tumor to bone marrow was improved from 10:1 to 30:1. **Conclusion:** This new method of WBIA yields significantly improved radioimmunotargeting of highly tumor-reactive, internalizing MAb BR96.

Key Words: tumor; rat; radioimmunotargeting; MAb BR96; immunoadsorption

J Nucl Med 1997; 38:895–901

Recently published results (*1,2*) concerning monoclonal antibody immunoconjugate BR96-doxorubicin (DOX) have generated a wave of enthusiasm among researchers and clinicians working with monoclonal antibodies (MAb) for cancer therapy (*3*). BR96 has high tumor selectivity, can rapidly internalize, has a direct cytotoxic effect on antigen-positive tumor cells and mediates both ADCC and CDC (*4*). The chimeric version of BR96 has the same properties as the native MAb but an even stronger antitumoral effect (*5,6*). Immunological studies have demonstrated that BR96 binds to differentiated epithelial cells of gastrointestinal tract and to a majority (>75%) of human carcinomas of breast, lung, ovary and gastrointestinal tract, expressing this antigen (*7*). Trail et al. (*1*) showed BR96-DOX to cure 94% of athymic rats with subcutaneous human lung carcinoma, even though these naked rats, like humans and in contrast to mice, expressed the BR96-target antigen in normal tissues although to a lesser extent than humans. On the other hand, several clinicians have shown some skepticism, pointing out that the preclinical data regarding MAb-based tumor targeting have not always been confirmed clinically (*8,9*). One argument is that studies of human tumors growing in immuno-compromised animals are not ideal for predicting antitumoral activity in the clinical setting. Moreover, in the case of drug conjugates that act stoichiometrically, a crucial factor is antigen density that should be very high to allow the intracellular localization of a sufficient number of cytotoxic molecules (*9*). When antigen expression is low or heterogeneous, as is usually the case in the clinical situation, conjugates with beta-emitting radionuclides may be more effective (*10*).

Extracorporeal immunoadsorption (ECIA) is a new method for selective removal of circulating radiolabeled monoclonal

antibodies (MAb) from plasma to increase the relative tumor uptake. Other groups have used ECIA by processing plasma through a goat antimouse MAb adsorbent column (11–13). Instead, we have experimentally applied a plasma-ECIA method based on the avidin-biotin concept (14–16). With such a method, a variety of selected MAbs can be removed from the circulation at a predetermined optimal interval after injection, provided that these MAbs are biotinylated. We have recently refined this method to enable whole-blood extracorporeal immunoadsorption (WBIA) and have shown it to be at least as efficient as plasma ECIA but also technically easier, safer and more reliable (17).

The primary aim of this study was to ascertain whether WBIA affects tumor and normal tissue radioimmunotargeting, that is to say improving the already high relative tumor uptake of BR96 MAb for the purpose of radioimmunotherapy. We have therefore investigated WBIA applied to chimeric BR96 in immunocompetent rats with a syngeneic tumor, a tumor model more closely imitating the human situation.

MATERIALS AND METHODS

Animals and Tumors

Forty-six immunocompetent Brown Norwegian (BN) male rats with a mean weight of 327 ± 19 g were transplanted with tumor cells from rat colon adenocarcinoma line BN7005 expressing Lewis Y (Le^Y) antigen. This tumor was originally induced by 1,2-demethylhydrazine in BN rats, which expresses the BR96 epitope in the pancreas and gastrointestinal tract, as well as in the tumor tissue (7). It was maintained with stable growth by serial passage in syngeneic rats of the BN line. The stem tumor was carefully homogenated and mixed with buffer solution at two ratios (1:1 for the LT or SRT; 1:8 for the IMT). Fifty microliters of the tumor suspension were then injected intramuscularly in the right thigh (IMT) and under the capsule of the two liver lobes (LT) or under the left kidney capsule (SRT). After 8 to 10 days, the xenografts had reached a mean weight of 0.28 ± 0.07 g (LT) and 0.39 ± 0.11 g in the SRT and IMT, respectively. To assess the extent of cellular and stromal components, four tumors were examined histologically using standard hematoxylin-eosin staining. The tissue specimens of the tumors were characterized by a carpet of undifferentiated adenocarcinoma cells with sparse vascularity and lacking a tumor capsule. Peripheral and central necrotic areas were more manifest in the IMT than in the LT.

One to two days before the WBIA procedure, the rats were catheterized with an arterial (a. carotis) and a venous (v. jugularis) catheter to gain blood access. The animals were provided with standard food pellets. The thyroid gland was not blocked, hence the uptake of free radioiodine in the gland could be observed.

Monoclonal Antibody, Radiolabeling and Biotinylation

The monoclonal antibody BR96 (Bristol Myers Squibb, Seattle, WA) is a chimeric of the human IgG$_1$ isotype and binds to a tumor-associated antigen closely related to Lewis-type (Le^Y) cell surface antigen. Six hundred micrograms BR96 were labeled with 18–20 MBq ^{125}I using the ATE method (18). Free iodine was separated from the MAb using a Sephadex G25 column (Pharmacia, Sweden). The ^{125}I-labeled BR96 was then conjugated with N-hydroxysuccin-imido-biotin (19). The amount of biotin reagent per milligram of BR96 was optimized to gain maximal cell binding activity in vitro in combination with maximal avidin binding. Forty-five micrograms of biotin reagent per milligram of BR96 MAb was used in the experiments. The radiolabeled and biotinylated BR96 was used within 1 day after labeling. A comparative biokinetic study of ^{125}I-BR96 and ^{125}I-BR96-biotin MAbs has
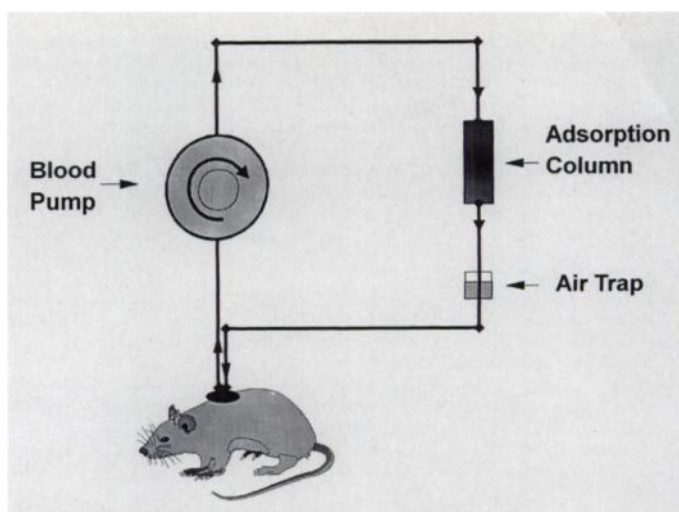
FIGURE 1. Schematic representation of extracorporeal immunoadsorption of whole blood (WBIA).

shown them to be similar concerning biodistribution both in tumors and normal tissues (Norrgren K, et al., *personal communication*).

Whole-Blood Extracorporeal Immunoadsorption

The principles of a plasma ECIA for removing exogenous targeting molecules have previously been described by our group (15,20). In this study, we explored a strategy for WBIA using an avidin-gel adsorption column (Fig. 1). This system allows direct adsorption of biotinylated MAb from unseparated blood and requires only a peristaltic blood pump, an adsorption column and connecting tubes with a drop-chamber (17). For the purpose of continuous extracorporeal blood circulation, a bypass should be used, omitting the adsorption column.

Just before the start of WBIA, the system was flushed with Buffer A, containing 20 IU/ml of heparin in order to prevent thrombotic complications and activation of the complement cascade. Blood was pumped from the arterial catheter through an adsorption column at a flow rate of 1.0 ml/min. In other words, approximately three plasma volumes were passed through the column and then returned through the drop chamber and the venous catheter to the rat. The adsorption column (1.5–2 ml) contained avidin covalently linked to CNBr (cyanogen-bromide)-activated sepharose 6MB macrobeads at a concentration of 2 mg avidin per milliliter gel. Before connection to the tubings, the column was carefully washed with 0.9% NaCl solution to eliminate free avidin from the adsorbent. In most of the experiments (n = 18), WBIA was started 12 hr after injection of ^{125}I-BR96-biotin and, in a limited number of experiments (n = 2), at 5 hr.

Experimental Design and Biodistribution Studies

The rats were divided into two groups: Group 1 (n = 26; controls given ^{125}I-BR96-biotin only and dissected at 7, 15 or 48 hr after injection of MAb) and Group 2 (n = 20; had WBIA at 5 or 12 hr after ^{125}I-BR96-biotin injection). The experimental design is shown in Figure 2. Forty-one BN rats were injected intravenously with 150 μg and five rats with 50 μg ^{125}I-labeled and biotinylated BR96 MAb (4.0–4.5 MBq). Animals in the WBIA and control groups receiving 50 μg BR96 manifested lower tumor uptake than those receiving 150 μg BR96. Thus, in all further experiments, the 150-μg dosage of BR96 was used. After the initial phase of the study, the SRT model was replaced by the LT model, which we consider to be a more feasible and appropriate model for the clinical situation. Blood samples were drawn as follows: immediately after the injection of BR96, just before the start of WBIA, in the middle of the procedure, immediately after termination of adsorption (i.e., before killing at 15 hr) and at 48 hr after the
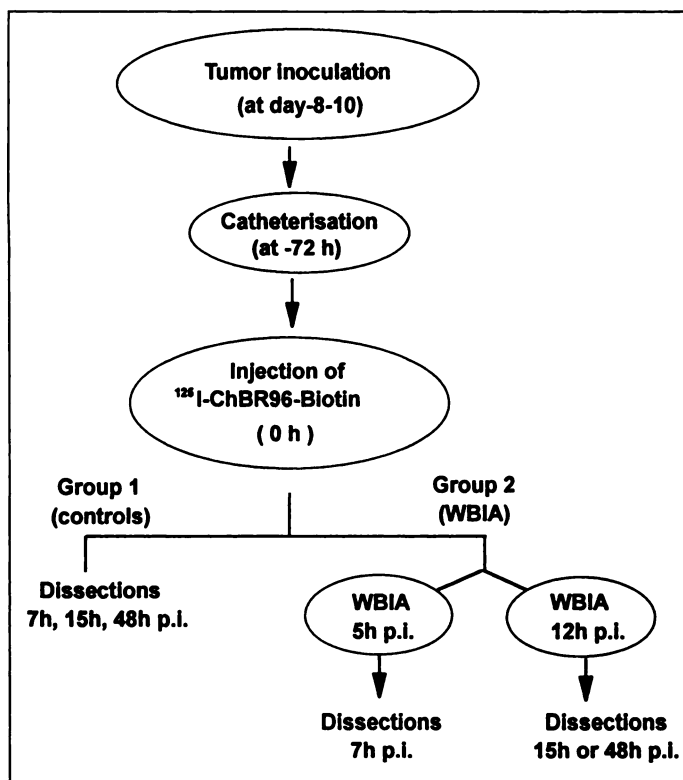
FIGURE 2. Experimental design.

injection of MAb (Fig. 2). The animals were killed after termination of the WBIA, apart from a group of four animals that was monitored for 33 hr after completion of the procedure (48 hr after injection of MAb). At dissection, the tumors in the liver, kidney and muscle (LT, SRT and IM, respectively) as well as several organs (bone marrow, liver, lungs, right kidney, thigh muscles, pancreas, bowel, spleen, stomach, lymph nodes and thyroid) were removed, weighed and measured for activity in an automatic well NaI counter. The activity uptake was expressed in percent of the injected activity per gram tissue (%/g), corrected for ^{125}I decay. Whole-body (WB) retention was registered immediately after injection of radioactivity before and after termination of WBIA or 48 hr after injection. A scintillation camera equipped with a low-energy parallel-hole collimator was used.

Quality Control of Radiolabeled MAb

After radiolabeling and biotinylation, the radioimmunoreactivity of the conjugate was tested against tumor cells. Approximately 20 ng of ^{125}I-BR96-biotin was mixed with a suspension of 2 × 10^8 DMHBN7005 cultured (ex vitro) or natural (ex vivo) tumor cells and incubated for 60 min at +2°C. After incubation, the cells were washed and measured for radioactivity in a NaI(Tl) well sample changer. Immediately before the injection, the free radioiodine concentration in the preparation of radiolabeled and biotinylated BR96, as well as the binding of the MAb to Avidin-Sepharose 6MB (2 mg/ml of settled gel), were tested.

Statistical Analysis

All the results are reported as means ± 1 s.d. The Lotus 1-2-3 Release 5.0 statistical program calculating sample statistics and a Student's t-test, assuming equal and unequal variances, was used to estimate mean differences. Confidence levels of more than 95% (p < 0.05) were considered to be significant.

RESULTS

Immediately before injection, the free radioiodine concentration in the preparation of radiolabeled and biotinylated BR96 was not higher than 5%, as verified with the TCA-precipitation method. The ^{125}I-labeling efficiency of BR96 MAb ranged from 45% to 48%, and radioimmunoreactivity assay confirmed binding capacity to the tumor cells to be 50%–55%. The binding of the biotinylated ^{125}I-MAb to avidin-sepharose 6MB reagent exceeded 85%.

Tumor Targeting

Activity uptake in tumors and normal tissues, expressed as percent of injected activity per gram tissue (%/g), was measured at 7 or 15 hr (just after completion of WBIA) and at 48 hr after injection of ^{125}I-BR96-biotin (Table 1). Peak tumor uptake was measured at 15 hr for all tumor sites. Highest uptake was found in LT followed in the order of size by SRT and IMT. In the control and WBIA groups, uptake in LT and IM tumors was less at 7 hr after injection than at 15 hr (Table 1). Both directly after completion of WBIA and 33 hr later (48 hr after injection of MAb), the activity uptake in the tumors was only noninsignificantly less than in corresponding controls (p > 0.05) and had approximately similar time-activity curves (Fig. 3). The reduction of activity uptake in LT was more pronounced when the procedure was started at 5 hr after injection of MAb.

TABLE 1
Uptake in Tumor and Normal Tissues Postinjection of Iodine-125-BR96-Biotin

| | 7 hr postinjection | | | | 15 hr postinjection | | | | 48 hr postinjection | | | |
| | WBIA | | Controls | | WBIA | | Controls | | WBIA at 12 hr | | Controls | |
Region	Avg.	s.d.	Avg.	s.d.	Avg.	s.d.	Avg.	s.d.	Avg.	s.d.	Avg.	s.d.
LT	1.98	0.13	2.47	0.14	5.06	1.19	5.39	1.46	2.61	0.15	2.98	0.39
IMT	1.04	0.06	0.92	0.15	1.39	0.32	1.38	0.36	1.20	0.29	1.14	0.14
SRT (n = 9)					2.90	0.83	3.85	0.55				
Plasma	1.2	0.1	6.3	0.5	0.9	0.2	5.3	0.7	1.2	0.2	2.5	0.2
Kidney	0.35	0.04	0.89	0.04	0.26	0.07	0.80	0.12	0.19	0.02	0.35	0.11
Liver	0.36	0.02	1.06	0.03	0.40	0.20	0.84	0.21	0.24	0.09	0.50	0.12
Pancreas	0.15	0.03	0.36	0.00	0.17	0.04	0.33	0.07	0.25	0.19	0.30	0.03
Bowel	0.19	0.02	0.30	0.15	0.13	0.03	0.29	0.15	0.13	0.02	0.20	0.03
Lung	0.42	0.02	0.73	0.01	0.37	0.07	0.89	0.19	0.32	0.04	0.51	0.10
Bone marrow	0.24	0.00	1.00	0.05	0.19	0.05	0.57	0.12	0.17	0.02	0.36	0.02

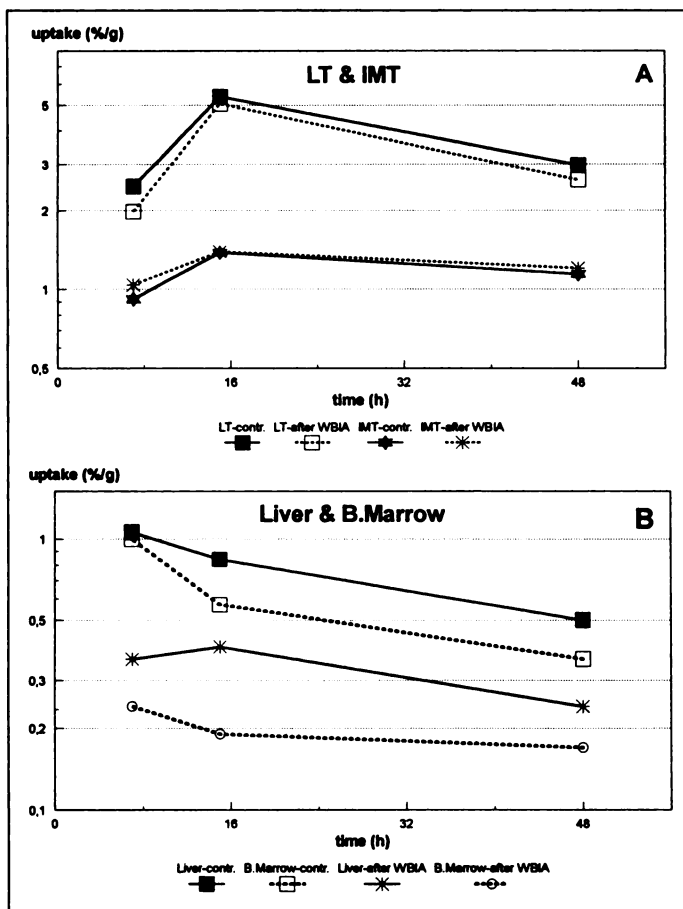LT = liver tumor; IMT = intramuscular tumor; SRT = subrenal capsula tumor.

FIGURE 3. (A) Activity uptake in tumors and (B) radiosensitive organs in WBIA and control groups.

FIGURE 4. (A) Whole-body and (B) plasma activity curves after injection of ^{125}I-BR96-biotin.

Normal Tissue Data

Normal tissue uptake of ^{125}I-BR96-biotin was modified by WBIA (Table 1). The notably low radioactivity of normal tissues in control rats was further reduced by WBIA. This was true both of organs sensitive to radiation and of the other tissues investigated. The activity uptake in bone marrow, liver, kidney, lung, pancreas and bowel directly after completion of WBIA was reduced by 40%–70%. During the next 33 hr (dissections 48 hr after injection), the uptake in normal organs was found to be 17%–53% less than in corresponding control rats (Table 1 and Fig. 3). In most of the normal organs, the reduction of radioactivity was more pronounced when the adsorption was started at 5 hr after injection. In relation to other normal tissues, radioactivity concentration in pancreas or bowel in which the epithelium can express BR96-target antigen was not increased either in the control group or in the WBIA group. The estimated total amounts of ^{125}I-BR96-biotin in the pancreas and the bowel of control rats at 15 hr postinjection were 0.19% and 0.37% of injected dose, respectively.

Whole-Body Retention

WBIA performed at 12 hr reduced the WB content from 82.2% to 41.2% or by 50.1% ± 5.4% (Fig. 4A). Further but slow decrease of WB activity from 41% to 37% was seen in rats monitored for another 33 hr after the completion of WBIA, which possibly indicates redistribution of the remaining activity after immunoadsorption. WB activity in control rats decreased more rapidly during the same time interval. However, 48 hr after injection, it was still about 20% higher than in corresponding WBIA animals. Immunoadsorption starting 5 hr after
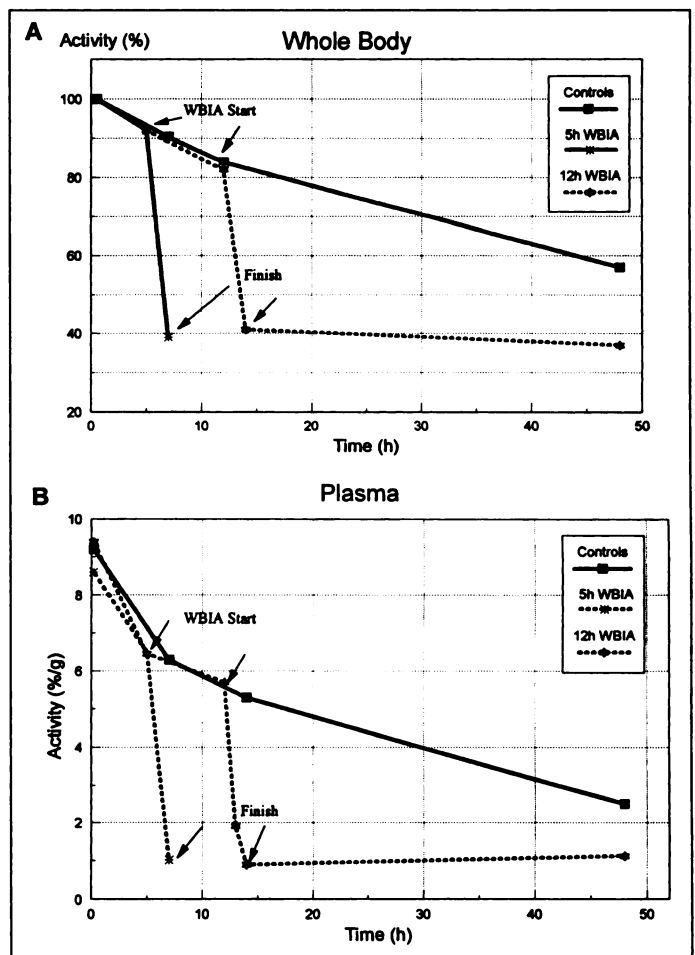
injection resulted in a reduction of WB activity from 93% to 40% at 7 hr, a reduction of 57%.

Plasma Clearance

The plasma activity concentration (%/g) at 12 hr after injection of MAb was as high as 59.5% ± 4.0% of the injected (Fig. 4B). As judged by pre- and postadsorption data, 85% of circulating plasma activity was removed by WBIA started at 12 hr: from 5.9% ± 0.7%/g to 0.9% ± 0.18%/g. WBIA starting at 5 hr after injection of MAb reduced plasma activity by 86% and thus was as effective as WBIA started 12 hr after injection. About 80% of the initial plasma activity was eliminated after the first hour after the start of WBIA. Clearance of the activity in control rat plasma continued to decrease after the injection of ^{125}I-BR96-biotin, whereas during another 33 hr after WBIA completion the plasma activity concentration increased from 0.9% ± 0.18%/g to 1.2% ± 0.16%/g due to equilibration between the blood and interstitial compartments. We previously observed this while using plasma immunoadsorption method with other MAbs (15,16).

Tumor-to-Normal Tissue

Uptake ratios are shown in Table 2. When WBIA was performed 12 hr after MAb injection, the LT-to-kidney uptake ratio was enhanced from 6.7 in the control group to 22.3 in the WBIA group, the corresponding increases being from 6.9–16.5 for the liver, from 6.4–14.9 for the lung and from 9.8–30.3 for bone marrow (p < 0.05). For the SRT, the corresponding increases were: 4.3–7.8 for the lungs, 4.6–7.3 for the liver, 4.8–11.1 for the kidneys and 6.8–15.2 for the bone marrow

TABLE 2
Liver Tumor-to-Tissue Ratios

	7 hr postinjection				15 hr postinjection				48 hr postinjection			
	WBIA		Controls		WBIA		Controls		WBIA		Controls	
	Avg.	s.d.	Avg.	s.d.	Avg.	s.d.	Avg.	s.d.	Avg.	s.d.	Avg.	s.d.
Kidney	5.7	1.0	2.8	0.1	22.3	11.3	6.7	1.6	11.1	1.6	5.8	1.4
Liver	5.5	0.7	2.3	0.1	16.4	8.9	6.9	2.6	9.2	1.9	4.7	0.9
Pancreas	14.1	4.0	2.5	0.1	33.7	7.6	18.5	2.2	7.5	3.3	7.0	1.1
Bowel	10.8	1.6	10.6	5.1	43.6	9.8	24.1	10.4	15.8	1.8	10.3	1.2
Lung	4.7	0.1	1.2	0.1	14.9	6.1	6.4	2.3	6.5	1.0	4.7	1.5
Bone marrow	8.2	0.5	2.5	0.1	30.3	15.1	9.8	3.5	12.3	1.8	6.4	1.5
Plasma	1.4	0.1	0.4	0.02	9.5	2.8	1.1	0.3	2.3	0.3	1.2	0.1

Intramuscular Tumor-to-Tissue Ratios

	7 hr postinjection				15 hr postinjection				48 hr postinjection			
	WBIA		Controls		WBIA		Controls		WBIA		Controls	
	Avg.	s.d.	Avg.	s.d.	Avg.	s.d.	Avg.	s.d.	Avg.	s.d.	Avg.	s.d.
Kidney	3.0	0.1	1.9	0.5	6.3	3.7	1.8	0.4	6.5	2.0	2.9	0.3
Liver	2.9	0.0	0.9	0.1	4.6	2.7	1.8	0.7	5.3	1.5	2.5	1.0
Pancreas	7.6	0.7	2.6	0.4	9.1	2.3	4.8	1.2	4.3	2.1	3.8	0.2
Bowel	5.7	0.1	3.6	1.3	11.8	3.0	7.6	5.1	8.4	1.4	5.7	1.2
Lung	2.3	0.1	1.3	0.2	4.1	1.6	1.7	0.6	3.8	1.2	2.3	0.2
Bone marrow	4.1	0.1	0.9	0.2	8.6	4.8	2.5	0.6	7.1	1.9	3.2	0.4
Plasma	0.9	0.11	0.15	0.02	1.5	0.41	0.30	0.06	1.0	0.18	0.51	0.07

(p < 0.05). For the IMT, the corresponding increases ranged from 1.6-fold for the bowel (p > 0.05) to 3.5-fold for the kidney and bone marrow (p < 0.01). When WBIA was started 5 hr after MAb injection, the enhancement of T/N uptake ratios was less pronounced, ranging from 35% to 77%. At 48 hr after injection, the T/N uptake ratios for the radiosensitive organs as bone marrow, liver and kidney were still 42%–78% higher in the WBIA groups than in corresponding control groups (p < 0.05).

According to our results, the radioactivity of blood cells is negligible, implying that the activity concentration in whole blood (%/g) is approximately half of the presented plasma levels (data on file). Based on plasma activity data (Table 2), the tumor-to-blood ratios in the control rats at 15 hr as well as at 48 hr postinjection exceeded the value of 2. As expected, these ratios were lower during the first hour after injection. Reduced whole-body radioactivity and improved immunoscintigraphic images of LT and IMT after WBIA are illustrated in Figures 5 and 6.

DISCUSSION

This study of tumor radioimmunotargeting with ^{125}I-labeled chimeric MAb BR96 in immunocompetent rats has shown this MAb to be characterized by a high degree of tumor selectivity. After WBIA, protracted enhancement of tumor-to-tissue uptake ratio was obtained as compared with control rats.

In the LT model, the tumor-to-bone marrow ratio was increased from 9.7:1 to 30.3:1 by using WBIA 12 hr after injection of MAb. The T/N ratios also improved significantly for the other radiosensitive organs (liver, kidney, lungs). In our studies, uptake of ^{125}I-BR96-biotin in liver tumors reached very high values (up to 7.4%/g), which are unusual in experimental radioimmunotargeting in rats. The LT is growing in a better vascularized organ than that of the IMT, and hence the former is probably more easily accessible for the antibodies used. Both the tumor models might, to a certain extent, reflect varying clinical situations with different conditions for tumor growth. Moreover, it should be borne in mind that, due to the differ-

ences in body weight and the initial concentration of MAb after intravenous injection (dilution effect), tumor uptake in the rats is approximately tenfold less than in mice. The uptake of irrelevant MAb L6 applied in the same model (in LT and IMT in two rats 12 hr after injection) was as low as 0.6%/g (data not presented here).

The uptake in all three tumors was not significantly reduced after the WBIA procedure, which might be partly explained by rapid internalization of BR96 MAb into lysosomes and endosomes (2,4,21). The rapid internalization is not only an important feature associated with a high therapeutic index of the antibody itself, but it is also very suitable when radioimmunotargeting is combined with WBIA. The radioactivity is then better retained in the tumor tissue, provided that the radionuclide and labeling method used are appropriate (22). The ATE radioiodine labeling method used in this study yielded consistent retention of ^{125}I in the tumor for at least 48 hr (19).

Another approach to the enhancement of T/N uptake ratios is the two-step strategy (23), such as injecting radiolabeled avidin, after the pretargeting of biotinylated MAb. However, this method cannot be used with internalizing MAbs.

The interval between MAb injection and the start of WBIA is a determinant of improvement of the T/N ratio and should be in agreement with the MAb uptake in tumor and normal tissue, as well as blood clearance rates (13). We assumed that, due to the fast biokinetics of ^{125}I-BR96-biotin, even higher T/N ratios might be attained if WBIA was started earlier than 12 hr after injection of MAb. However, our pilot study of WBIA performed as early as 5 hr after injection of MAb did not confirm any improvement in terms of T/N ratios. Hence, the optimal time for starting immunoadsorption of ^{125}I-BR96-biotin in rats is probably in the interval 5–12 hr after MAb injection. Extrapolated to humans, the start time of WBIA might depend on many factors, such as activity distribution in tumor, blood and normal tissue, which should be determined individually before RIT.
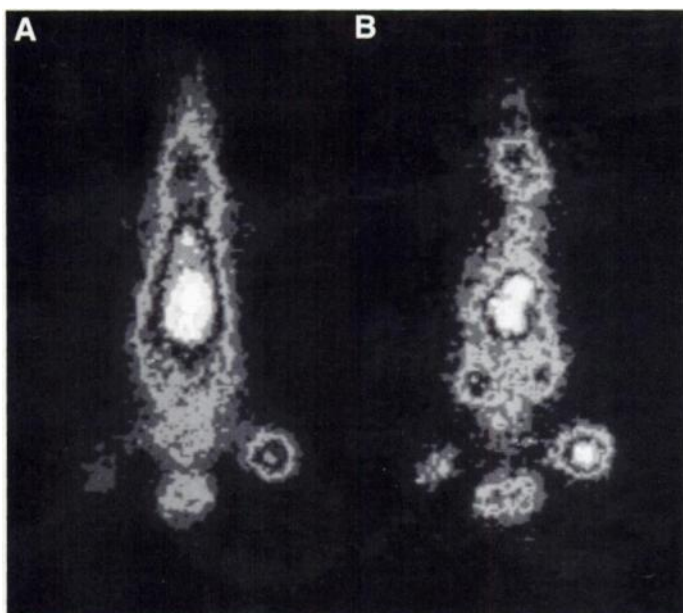
FIGURE 5. Radioimmunoscintigrams of a rat before WBIA (A) 12 hr after injection of ^{125}I-BR96-biotin and (B) immediately after completion of the procedure 15 hr after injection. WBIA reduced whole-body radioactivity and improved liver tumor imaging.

A general limitation of the human xenografted mouse model, which continues to be the one most frequently used, is the oversimplification of the preclinical experimental system. Even target antigens that are not tumor specific in humans become unique antigens in mice whose normal tissues do not express the relevant antigen (9). The rat model fully mimics the human situation as rats manifest a tissue distribution of the selected antigen (Le^y) very similar to that in humans (1). Accordingly, it is preferable to use a rat model rather than a mouse model to adequately evaluate tissue distribution and the therapeutic potential of BR96.
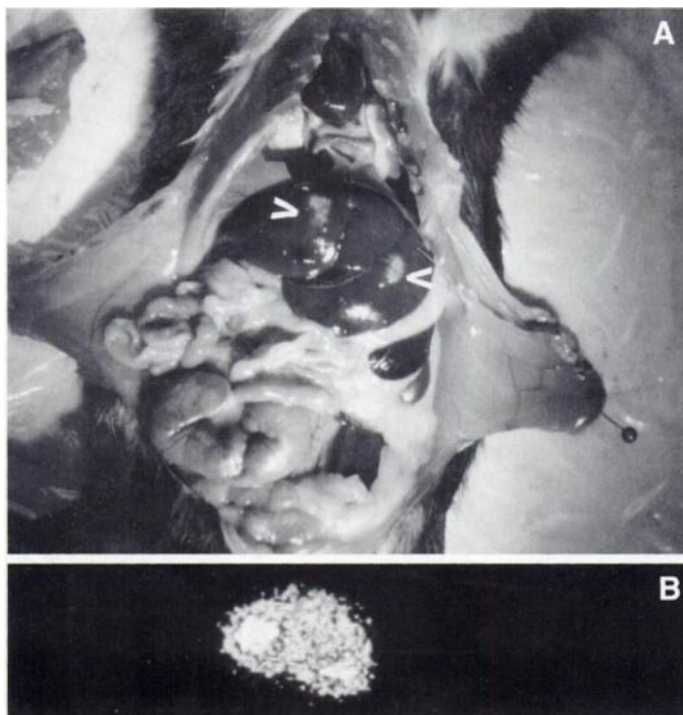
FIGURE 6. (A) A rat under dissection with two syngeneic liver tumors of 250–300 mg each and (B) an ex-vivo radioimmunoscintigram of the same liver after WBIA 12 hr after injection of MAb.

The low uptake of ^{125}I-BR96-biotin in tissue samples from stomach, bowel and pancreas was unexpected as Le^y Ag is expressed in differentiated epithelial cells of gastrointestinal tract and of accinar cells in the pancreas (1). The explanation might be that the Le^y Ag is expressed in the apical parts of the cells adjacent to the exocrine lumen and is thus not exposed to the circulation that is a prerequisite for internalization of the MAb (21). Trail et al. (1) have shown that BR96-DOX cures 94% of athymic rats with subcutaneous human lung carcinoma. To be effective, drug and toxinimmunoconjugates need to be taken up by each cell and transferred to the cytosol. Isaksson et al. (24) showed that BR96-DOX conjugate therapy of well-established intrahepatic or subcutaneous growth of BR96-positive tumors (expressing binding activity) to yield cures in approximately 50% of the animals, whereas therapy of analogous intrahepatic tumors containing an admixed variant of BR96-negative tumor cells among a majority of BR96-positive cells showed continued outgrowth of the BR96-negative cells, despite a complete eradication of the BR96-positive cells. The use of drugs is thus limited in the clinical situation, as most tumors manifest heterogeneity of antigen expression. MAb labeled with beta-minus emitters (e.g., ^{131}I) can, however, distribute their cytotoxicity to antigen-negative cells from neighboring antigen-positive cells. Doxorubicin might also depress the cell-mediated immunological effects. Acquired multidrug resistance of tumor cells is another obstacle to the use of drug and toxinimmunoconjugates in the clinical situation.

CONCLUSION

This study showed that a new method of WBIA was applicable on the internalizing, highly tumor-reactive MAb BR96, resulting in manifestly improved radioimmunotargeting. After completion of WBIA, a protracted enhancement of T/N uptake ratios was obtained as compared to control rats.

REFERENCES

1. Trail PA, Willner D, Lasch SJ, et al. Cure of xenografted human carcinomas by BR96-doxorubicin immunoconjugates. Science 1993;261:212–215.
2. Garrigues J, Garrigues U, Hellström I, Helström K-E. Le^y specific antibody with potent antitumor activity is internalized and degraded in lysosomes. Am J Pathol 1993;142:607–622.
3. D'Incalci M. Immunoconjugates. The magic bullet revisited or future tumor-targeting therapy? Ann Oncol 1994;5:697.
4. Hellström I, Garrigues HJ, Garrigues U, Hellström K-E. Highly tumor-reactive, internalizing, mouse monoclonal antibodies to Le (y)-related cell surface antigens. Cancer Res 1990;50:2183–2190.
5. Schreiber GJ, Hellström K-E, Hellström I. An unmodified adenocarcinoma antibody, BR96, localizes to and inhibits the outgrowth of human tumors in nude mice. Cancer Res 1992;52:3262–3266.
6. Yarnold S, Fell HP. Chimerization of antitumor antibodies via homologous recombinant conversion. Cancer Res 1994;54:506–512.
7. Casazza AM, Trail PA, Hellström K-E. Drug immunotargeting for carcinomas: a reality at last? Ann Oncol 1994;5:703–708.
8. Colnaghi MI, Menars S, Canevari S. Evolution of the therapeutic use of new monoclonal antibodies. Curr Opin Oncol 1993;5:1035–1042.
9. Canevari S, Colombatti M, Colnaghi MI. Immunoconjugates: lessons from animal models. Ann Oncol 1994;5:698–701.
10. Goldenberg DM. Monoclonal antibodies in cancer detection and therapy. Am J Med 1993;94:297–312.
11. Johnson TK, Maddock S, Kasliwal R, et al. Radioimmunoadsorption of KC-4G3 Ab in peripheral blood: implications for radioimmunotherapy. Antibody Immunoconj Radiopharm 1991;4:885–893.
12. Dienhart DG, Kasliwal R, Lear JL, et al. Extracorporeal immunoadsorption of radiolabeled monoclonal antibody: a method for reduction of background radioactivity and its potential role during the radioimmunotherapy of cancer. Antibody Immunoconj Radiopharm 1994;7:225–252.
13. DeNardo G, Maddock SW, Sgouros G, Scheibe PO, DeNardo SJ. Immunoadsorption: an enhanced strategy for radioimmunotherapy. J Nucl Med 1993;34:1255–1262.
14. Strand S-E, Norrgren K, Ingvar C, Erlandsson K, Persson EC. Plasmapheresis as a tool for enhancing contrast in radioimmunoimaging and modifying absorbed doses in radioimmunotherapy [Abstract]. Med Phys 1989;16:465.
15. Norrgren K, Strand S-E, Nilsson R, Lindgren L, Sjögren HO. A general extracorporeal immunoadsorption method to increase tumor-to-normal tissue ratio in radioimmuno-imaging and radioimmunotherapy. J Nucl Med 1993;34:448–454.
16. Garkavij M, Tennvall J, Strand S-E, et al. Improving radioimmunotargeting of tumors: variation in the amount of L6 MAb administered, combined with an immunoadsorption

system (ECIA). *Acta Oncol* 1993;32:853–859.
17. Garkavij M, Tennvall J, Strand S-E, et al. Extracorporeal immunoadsorption (ECIA). from whole blood based on avidin-biotin concept: evaluation of a new methodical approach. *Acta Oncol* 1996;35:309–312.
18. Zalutsky MR, Noska MA, Colapinto EV, et al. Enhanced tumor localization and in vivo stability of a monoclonal antibody radioiodinated using N-succinimidyl 3-(tri-n-butylstannyl) benzoat. *Cancer Res* 1989;49:5543–5549.
19. Chen J, Strand S-E, Sjögren H-O, et al. Pharmacokinetic and biodistribution studies of paired-labeled ChiBR96 in colon carcinoma isotransplanted rat: potency of the use of extracorporeal immunoadsorption to increase the uptake ratio of tumor-to-tissue [Abstract]. *Proceedings of the Fourth Scandinavian Symposium on Radiolabeled Monoclonal Antibodies in Diagnosis and Therapy of Cancer*. Lillehammer, Sweden: 1995:7–8.
20. Norrgren K, Garkavij M, Lindgren L, et al. Evaluation of the extracorporeal immunoadsorption on the biokinetics of ^{125}I-labeled monoclonal antibody L6 in a nude rat model. *Antibody Immunoconj Radiopharm* 1994;7:29–42.

21. Siegall CB, Chase D, Mixan B, et al. In vitro and in vivo characterization of BR96sFv-PE40. A single-chain immunotoxin fusion protein that cures human breast carcinoma xenografts in athymic mice and rats. *J Immunol* 1994;3:2377–2384.
22. Stein R, Goldenberg DM, Thorpe SR, et al. Effects of radiolabeling on monoclonal antibodies with a residual iodine radiolabel on the accretion of radioisotope in tumors. *Cancer Res* 1995;55:3132–3139.
23. Khawli LA, Alauddin MM, Miller GK, et al. Improved immunotargeting of tumors with biotinylated monoclonal antibodies and radiolabeled streptavidin. *Antibody Immunoconj Radiopharm* 1993;6:13–27.
24. Isaksson M, Trail PA, Nilsson R, Helström I, Helström K-E, Sjögren HO. Use of the BR96-DOX immunoconjugate in immunotherapy against established intrahepatic tumors in an immunocompetent rat colon carcinoma model [Abstract]. In: *Proceedings of the Fifth International Conference on Anticancer Research*. Corfu, Greece: 1995:21.

Rapid Imaging of Experimental Infection with Technetium-99m-DTPA After Anti-DTPA Monoclonal Antibody Priming

Marion H.G.C. Kranenborg, Wim J.G. Oyen, Frans H.M. Corstens, Egbert Oosterwijk, Jos W.M. van der Meer and Otto C. Boerman

Departments of Nuclear Medicine, Urology and Internal Medicine, University Hospital Nijmegen, The Netherlands

Antibodies accumulate nonspecifically in infectious foci due to the locally increased vascular permeability. This study describes a method of infection imaging in which ^{99m}Tc-DTPA (diethylenetriaminepentaacetic acid) is trapped at the target by a previously administered anti-DTPA monoclonal antibody, DTIn1. **Methods:** Rats with *Staphylococcus aureus*-infected calf muscle were injected intravenously with DTIn1. Two to 24 hr after the DTIn1 injection, ^{99m}Tc-DTPA was injected intravenously. In separate experiments, excess DTIn1 was cleared from the circulation 2 hr after injection with bovine serum albumin (BSA)-DTPA-In, galactosylated BSA-DTPA-In, goat antimouse IgG or avidin. Additionally, the effect of DTIn1 dose on ^{99m}Tc-DTPA abscess uptake was determined in a three-step protocol. The distribution of the radiolabels was studied by γ counting of dissected tissue and gamma camera imaging. **Results:** Priming with DTIn1 resulted in specific retention of ^{99m}Tc-DTPA in the abscess. Such ^{99m}Tc-DTPA abscess uptake was not dependent on the interval between the DTIn1 and the ^{99m}Tc-DTPA injection: Optimal ^{99m}Tc-DTPA abscess uptake was already achieved within a 2-hr time span between the DTIn1 and DTPA injections. However, relatively high ^{99m}Tc-DTPA background was observed due to slowly clearing DTIn1-^{99m}Tc-DTPA complexes. Background reduction with various agents had a prominent effect on DTIn1 as well as ^{99m}Tc-DTPA biodistribution. The best reduction was obtained using BSA-DTPA-In. Optimal ^{99m}Tc-DTPA abscess uptake in the three-step protocol was obtained at higher DTIn1 doses (>100 µg). **Conclusion:** Infectious foci in a rat model can be imaged earlier with extremely low background levels after priming with DTIn1, followed by BSA-DTPA-In and imaging with ^{99m}Tc-DTPA, as compared with directly labeled IgG.

Key Words: technetium-99m-DTPA; monoclonal antibody priming; infection imaging; pretargeting protocols

Scintigraphic imaging of focal infection is currently performed with various agents, such as ^{67}Ga-citrate, radiolabeled leukocytes or ^{111}In-labeled human IgG (*1,2*). Large proteins such as IgG and human serum albumin localize nonspecifically in infectious and inflammatory foci due to the locally enhanced

vascular permeability (*3,4*). Although labeled IgG is a convenient radiopharmaceutical, its relatively slow blood clearance, which causes persistently high background activity, interferes with the early diagnosis of infection and inflammation (*5*).

Reduction of background activity may be accomplished by pretargeting protocols. In these methods, the infectious focus is pretargeted and the radionuclide is administered afterwards as a low molecular weight ligand. The small ligand is rapidly excreted when not targeted to the infectious focus. Streptavidin and biotin have been used in such multistep approaches (*6–8*). Rusckowski et al. pretargeted mice with *Escherichia coli* infection with cold streptavidin and injected ^{111}In-biotin 3 hr later (*8*). Higher abscess-to-background ratios were obtained compared with ^{111}In-streptavidin or ^{111}In-IgG. Similar results were observed in tumor pretargeting studies using antichelate antibodies and radiometal labeled chelates (*9–12*).

In this study, we investigated a multistep strategy for rapid infection imaging using an anti-DTPA (diethylenetriaminepentaacetic acid) monoclonal antibody (MAb) as the pretargeting agent and ^{99m}Tc-DTPA as the targeting radiopharmaceutical.

MATERIALS AND METHODS

Radiopharmaceuticals

Technetium-99m-IgG. Human nonspecific IgG in kit form (Technescan-HIG; Mallinckrodt Medical B.V., Petten, The Netherlands) was labeled with 750 MBq ^{99m}Tc eluate according to the manufacturer's instructions.

Monoclonal Antibodies. The production of anti-DTPA MAb DTIn1 (IgG2a), reacting with DTPA loaded with different metals, has been described (*13*). The affinity constant for ^{99m}Tc-DTPA was approximately 0.2 nM^{-1}, which is similar to that for ^{111}In-DTPA (*13*). The IgG2a switch variant of MAb G250 (*14*) was used as a non-DTPA binding-control antibody. DTIn1 and G250 were labeled with ^{125}I (Amersham International, Buckinghamshire, U.K.) using the Iodogen method (*15*).

Biotinylated DTIn1. DTIn1 was conjugated with NHS-LC-biotin (Pierce, Rockford, IL). Briefly, 0.8 mg DTIn1 and 740 µg NHS-LC-biotin in 50 mM sodium phosphate (pH 7.5) were incubated for 16 hr at 4°C. Thereafter, unreacted biotin was removed by PD10 (Pharmacia LKB Technology, Uppsala, Sweden) chromatography. Each DTIn1 molecule contained 18